STUDY ON IMPACT PROPERTIES OF CREEP-RESISTANT STEEL THERMALLY SIMULATED HEAT AFFECTED ZONE

by

Radivoje M. MITROVIĆ [a], ***Dejan B. MOMČILOVIĆ*** [b], ***Olivera A. ERIĆ*** [*c], ***Ivana D. ATANASOVSKA*** [c], ***and Nenad T. HUT*** [b]

[a] Faculty of Mechanical Engineering, University of Belgrade, Belgrade, Serbia
[b] Institute for Testing of Materials IMS, Belgrade, Serbia
[c] Institute "Kirilo Savić", Belgrade, Serbia

Original scientific paper
DOI: 10.2298/TSCI111006142M

The steam pipe line and steam line material, along with its welded joints, subject to damage that accumulates during operation in coal power plants. As a result of thermal fatigue, dilatation of steam pipe line at an operating temperature may lead to cracks initiation at the critical zones within heat affected zone of steam pipe line welded joints.
By registration of thermal cycle during welding and subsequent heat affected zone simulation is possible to obtain target microstructure. For the simulation is chosen heat resisting steel, 12H1MF (designation 13CrMo44 according to DIN standard). From the viewpoint of mechanical properties, special attention is on impact toughness mostly because very small number of available references. After simulation of single run and multi run welding test on instrumented Charpy pendulum. Metallographic and fractographic analysis is also performed, on simulated 12H1MF steel from service and new, unused steel. The results and correlation between microstructure and impact toughness is discussed, too.

Key words: *heat resisting steel, heat affected zone, instrumented Charpy test, impact toughness*

Introduction

Steam pipe lines undergo very complex service conditions, fatigue-creep and low cycle thermal fatigue at elevated temperatures, and, from a safety aspect, are the very significant system of a coal power plants.

Therefore, the steam pipe line (SPL) and steam line material, along with its welded joints, subject to damage that accumulates during operation which can lead to fracture.

From the standpoint of energy efficiency, these accumulations of damage make a vital understanding of all influential factors that contribute to degradation of material properties over longer period of time [1].

There are two main causes of degradation of material properties of steam pipe lines SPL:

– interaction between fatigue-creep (low cycle and thermal fatigue), and

* Corresponding author; e-mail: olivera66eric@gmail.com

– primary stresses induced by the weight of the steam line itself, noted above, and the influence of hangers on secondary induced stresses [2].

As a result of thermal fatigue, dilatation of SPL at an operating temperature may lead to cracks initiation at the critical zones within heat affected zone (HAZ) of welded joints [3]. We should not forget the residual stresses due to welding that can be superimposed with operating stresses, and can also be induce initiation of cracks [4, 5]. It is necessary to mention the corrosion and stress corrosion as another possible cause of initiation of cracks in the steam line [6, 7]. However, the most significant effect on the occurrence of damage and reduction of SPL service life of materials has the appearance of creep [8].

Development of material damage during the operation is followed by the continuous creation of cavities or micropores at grain boundaries. Many authors state that the cavities were present before the process of creep, as a result of SPL steel production process. Regardless of background, the cavities grow during creep [9, 10]. Cavity size is largely dependant also on material type, however it is in the range of micron size (often also lower), therefore they are usually called "microvoids" or "micro-cavities". One of the basic acceptance tests of welds and HAZ is impact energy test by Charpy method. The classic energy impact testing, without separation of energy initiation and energy propagation of crack during the tests, does not give a complete view situation of the impact strength of the tested material. Therefore, in these studies, it is necessary to use instrumented Charpy pendulum [11, 12].

Knowledge of the microstructure and their variations with different thermal cycles of welding and impact energy dependence of the microstructure, can be obtained by improving the welding parameters during welding repair on the one hand, and making assessment of the existing welds from the point of remaining service life, energy efficiency and behavior of welded joints during accidental situations, on the other hand [13].

By registering during welding thermal cycle, during welding of full scale pipe, and then simulating obtained welding cycle on simulators, on samples of material from which the SPL is made, it is possible to obtain the desired microstructure corresponding to the selected critical microstructure within the HAZ, but in dimensions sufficient for reliable testing of destruction which is the aim this paper.

Experiment

Methodology and equipment

Today, welding simulators are used to determine mechanical properties of the "weakest link" *i. e.* critical microstructure within a HAZ. Welding simulator (fig. 1) is a device that achieves controlled heating and cooling similar to the thermal cycle during welding. The difference is in obtained micro structure, on a sample size of $10 \times 10 \times 60$ mm, and at its middle part, as microstructure which corresponds to the desired critical area. The critical area of HAZ is usually coarse grain zone, and simulation enables the exact identification of fundamental mechanical properties [14, 15]. Input parameters are performed via computer, and selection of the basic parameters can be determined from the calculation of the temperature field or by the using of appropriate equations to calculate $\Delta t_{8/5}$ in the welding thermal cycle [16]. The origin of the parameters can be also experimental obtained, by measuring the thermal cycle with the thermocouples.

In order to obtain experimental values comparable with existing from literature (and each other), for testing was selected (and sampled steel) from exploitation (marked as old pipe – OP), and a new unused steel pipe (marked as new pipe – NP).

In both cases, the used steal was 12H1MF according to GOST 20072-74, [17]. In both group of specimens, samples were cut from the tube diameter Ø245 × 22 mm. Basic data for OP group of specimens, taken from the coal power plant is the working temperature of 509-520 °C, working pressure 130 bar and 230 start-up, with a total of 72,000 hours spent in service.

Figure 1. Heat affected zone simulator SMITWELD

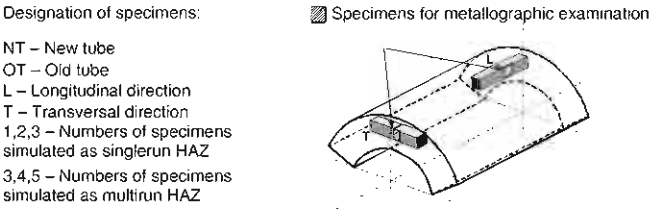

Figure 2. Schematic presentation of specimens sampling from SPL tubes

Orientation and labeling of samples measuring 11 × 11 × 60 mm is shown in fig. 2. As can be seen from fig. 2, samples are labeled L (longitudinal) and T (transversal), which indicate the position on the tube wall thickness. Tube numbers 1-3 indicate the simulated samples as a single run welding of tubes, while numbers 3-5 indicate the simulated samples as multi run welding.

In order to perform characterization of simulated specimens, the following tests were completed:

(1) examination of the chemical composition for each group of tubes,
(2) simulation of HAZ;
(3) hardness measurement in the zone -working part of the tube,
(4) examination of the impact energy with a instrumented Charpy pendulum SCHENCK TREBEL 300,
(5) metallographic examination close to the fracture site in the working part of the tube below the point, fig. 2 hatched area, and
(6) fractography examination of a breaking surface tubes with a scanning electron microscope (SEM) Phillips 515.

The sequence of tests above is also the methodology and reliable determination of the tested impact toughness characteristics of the critical areas within the HAZ.

HAZ simulation parameters

Simulation of steel 12H1MF samples was performed on the simulator Smitweld LS1402, on the Welding Institute in Timisoara, Romania. A simulation of thermal cycles and thermal treatment was carried out for all these combinations of specimen groups, NP-L, NP-T, OP-L, and the OP-T:

– the constant heating rate until reaching the maximum temperature of the cycle – P_t for 10s;
– cooling rate in the range of 800-500 °C, according to the thickness of 22 mm, of the upper limit of $T/t_{8/5}$ = 30 °C/s which corresponds to $t_{8/5}$ = 10 seconds;
– The maximum temperature in the simulated cycle, in the case of a single run welding P_t = 1350 °C (designation: single pass simulation – SPS),
– Maximum temperatures in the simulated cycle, in the case of a multi run welding P_t = 1300 °C, 1200 °C, and 1000 °C (designation: multi pass simulation – MPS), and
– Thermal treatment after conducted simulation of multi layer welding at 500 °C for 3 hours.

After simulation of samples with dimensions 11 × 11 × 60 mm, standard Charpy specimens were made according to EN 10045-1, with the standard V notch.

Base material properties

The chemical composition of tested samples correspond with the standard requirements, tab. 1. The results of mechanical properties testing are presented in tab. 2. Obtained results are above minimal required values by standard GOST 20072/74 [17].

Table 1. Chemical composition of 12H1MF according to GOST 20072/74

C [%]	Si [%]	Mn [%]	S [%]	P [%]	Cr [%]	V [%]	Mo [%]	Cu [%]	Ni [%]
0.08-0.15	0.17-0.37	0.40-0.70	0.025	0.030	0.90-1.20	0.15-0.30	0.25-0.35	0.20 max.	0.30 max.

Table 2. Mechanical properties of 12H1MF according to GOST 20072-74

Yield strength R_e [MPa]	Tensile strength R_m [MPa]	Elongation A_5 [%]	Impact toughness on + 20 °C KV [J]	Vickers hardness HV5
239	434	24,3	59	117

Results

Hardness testing

Hardness measurement, HV5, was performed on the Charpy specimens according to standard EN ISO 6507-1:2005. The scheme of hardness measurement is shown in fig. 3. The results of hardness measurements are shown in tab. 3.

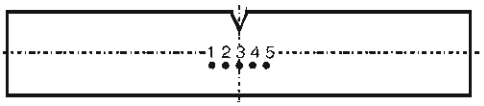

Figure 3. Hardness measurement points on Charpy specimens with 2 mm depth V notch

Table 3. The results of hardness measurements

Sample	Simulation of welding	HV5				
		1	2	3	4	5
NP-L	SPS	321	303	306	280	283
	MPS	317	313	303	303	303
NP-T	SPS	293	321	286	299	298
	MPS	272	276	257	280	280
OP-L	SPS	243	232	252	232	232
	MPS	164	172	175	106	146
OP-T	SPS	220	241	199	232	241
	MPS	220	210	202	210	210

Impact toughness (Charpy) testing

Examination of the impact energy was carried out on Charpy instrumented pendulum, with maximum impact energy of 300 J. That made possible to determine not only the total, but also initiation and propagation energy of the tested material. Test results are shown in tabs. 4-7.

In fig. 4, the typical force-time diagrams of samples, are presented.

Table 4. The results of impact energy for the sample group NP-L

Mark of group of samples, numbers of specimens and maximal temperature of thermal cycle		Initiation energy KV [J]	Propagation energy KV [J]	Total energy KV [J]	Average value KV [J]
NP-L	SPS (1350 °C)	13.0	12.6	25.6	40.1
		34.0	11.8	45.8	
		40.0	8.8	48.8	
	MPS (1300 °C, 1200 °C, 1000 °C)	80.0	42.8	128.0	116.2
		65.0	19.4	84.4	
		90.0	46.3	136.3	

Table 5. The results of impact energy for sample group NP-T

Mark of group of samples, numbers of specimens and maximal temperature of thermal cycle		Initiation energy KV [J]	Propagation energy KV [J]	Total energy KV [J]	Average value KV [J]
NP-T	SPS (1350 °C)	9.0	4.7	13.7	15.3
		12.0	6.8	18.8	
		9.0	4.5	13.5	
	MPS (1300 °C, 1200 °C, 1000 °C)	251	34.1	59.2	52.7
		25.0	29.8	54.8	
		30.0	24.2	44.2	

Table 6. The results of the impact energy for the sample group OP-L

Mark of group of samples, numbers of specimens and maximal temperature of thermal cycle		Initiation energy KV [J]	Propagation energy KV [J]	Total energy KV [J]	Average value KV [J]
OP-L	SPS (1350 °C)	41.0	8.8	49.8	30.0
		14.0	8.6	22.6	
		15.0	2.7	17.7	
	MPS (1300 °C, 1200 °C, 1000 °C)	65.0	96.0	161.0	152.9
		60.0	93.2	153.2	
		60.0	84.9	144.9	

Table 7. The results of impact energy for the sample group OP-T

Mark of group of samples, numbers of specimens and maximal temperature of thermal cycle		Initiation energy KV [J]	Propagation energy KV [J]	Total energy KV [J]	Average value KV [J]
OP-T	SPS (1350 °C)	6.0	120	18.0	30.0
		12.0	22.1	34.1	
		6.0	7.4	13.4	
	MPS (1300 °C, 1200 °C, 1000 °C)	14.0	46.4	60.4	52.1
		15.0	21.9	36.9	
		12.0	47.0	59.0	

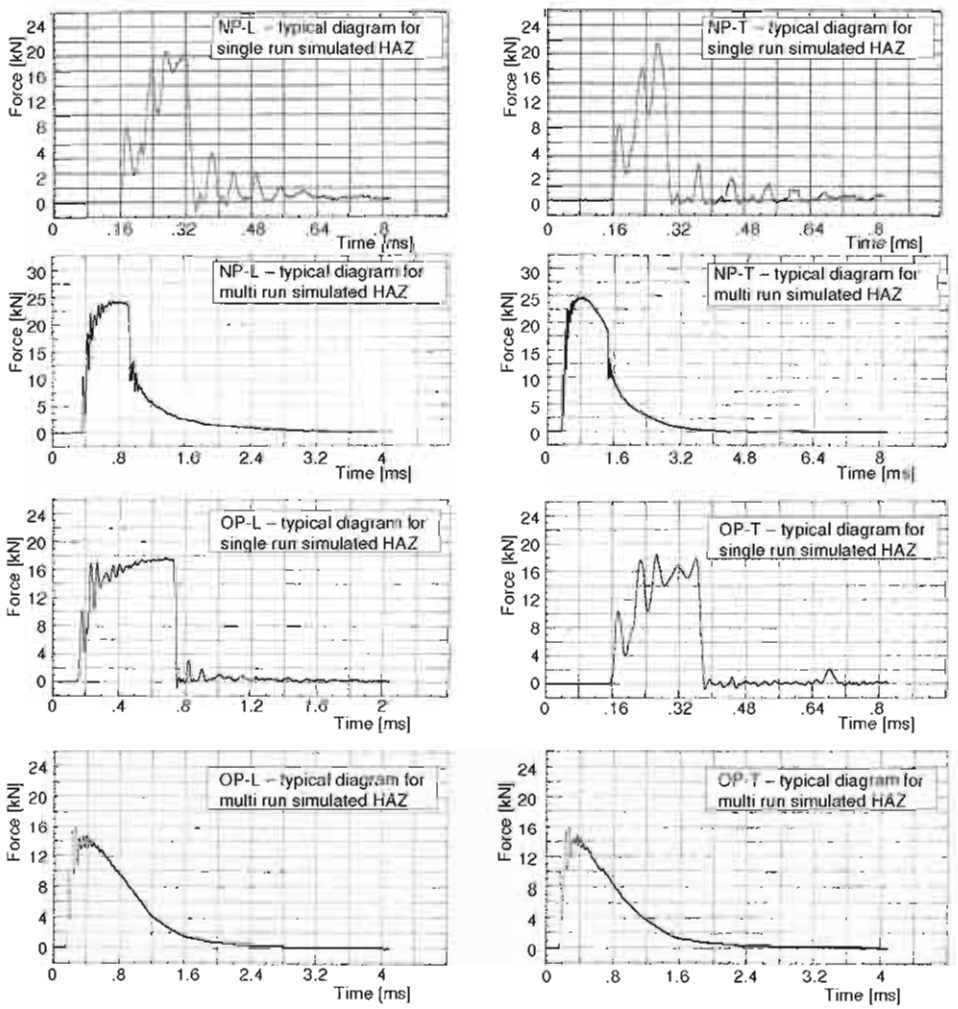

Figure 4. The appearance of characteristic force-time diagram

The results of metallographic examination by light microscopy (LM)

The samples for metallographic examination are made from broken specimens after Charpy impact test. Reviewed places are schematically indicated in fig. 2. Microstructure of samples NP-L and OP-L are shown in figs. 5 and 6. As the initial microstructure and the microstructure after the simulations were identical on samples for testing both directions (L and T) groups, it will be shown only to characteristic microstructures.

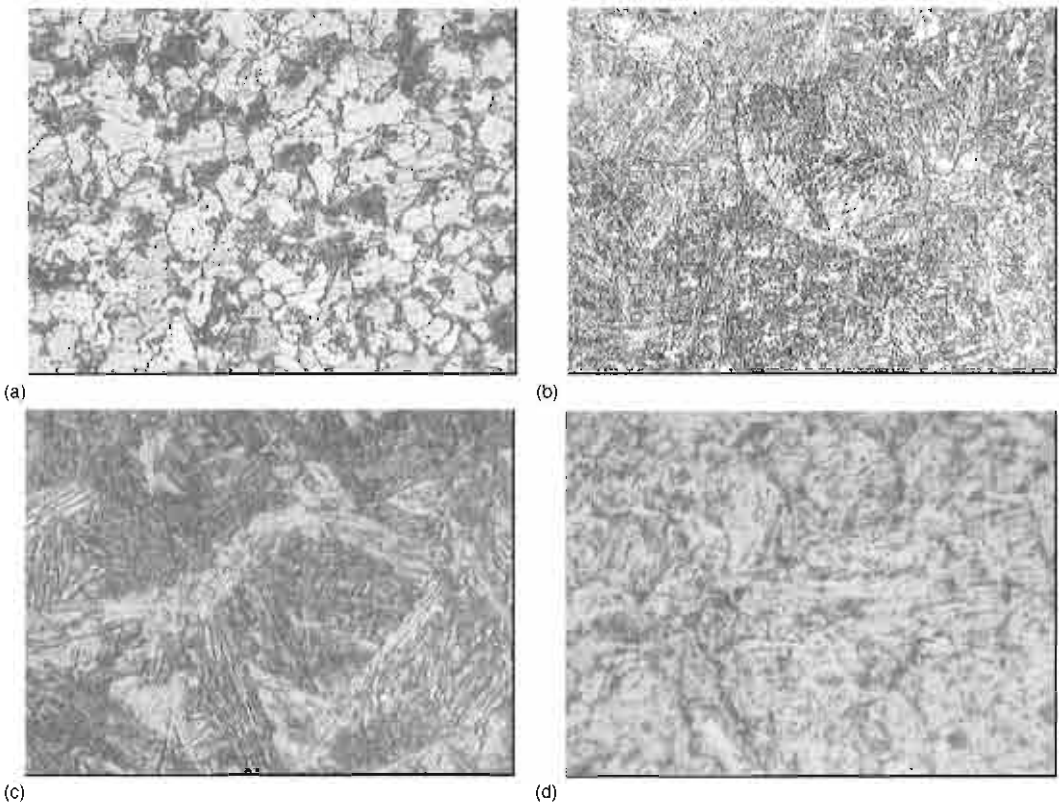

Figure 5. The microstructures of samples from NP-L group;
(a) – base material, ferrite pearlite structure, ×400, (b) – HAZ, single run welding simulated HAZ, ×400, (c) – detail from the picture 6(b) single run welding, the ferrite on bainite grain boundaries, ×1000, (d) – multi run welding, ferrite – bainite structure ×400

SEM examination

The fractured surfaces of the broken Charpy specimens were examined with a SEM Phillips 515. Figures 7 and 8 show the microstructure samples of OP-L and NP-L group.

Discussion

Hardness measurements on the samples of NP-L and OP-L (tab. 3), shows that the measured values of hardness at the multi run welding are higher than on single run welding.

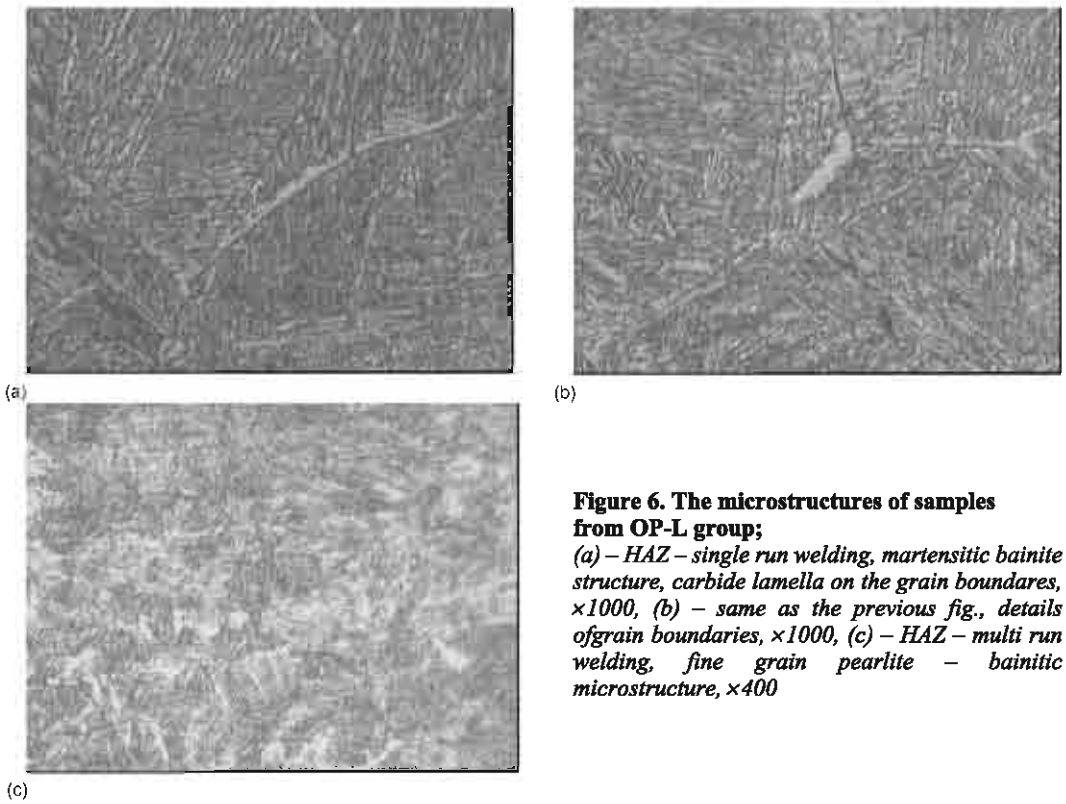

Figure 6. The microstructures of samples from OP-L group;
(a) – HAZ – single run welding, martensitic bainite structure, carbide lamella on the grain boundares, ×1000, (b) – same as the previous fig., details ofgrain boundaries, ×1000, (c) – HAZ – multi run welding, fine grain pearlite – bainitic microstructure, ×400

Based on the examination carried out in both groups of NP and OP specimens, it can be seen that the tubes sampled from the longitudinal direction have higher values of impact energy in comparison to the sampling tubes from the transversal direction. The elongated microstructure which would indicate that higher impact energy values in longitudinal direction, was not confirmed or found neither in the simulated HAZ nor in the base material. However, a significant amount of lamination caused by residual non-metallic inclusions observed in figs. 7, (b), (c) and (e), indicate that there was a "lamination strengthening", since their great number is observed. The influence of inclusions on the overall energy impact is negative. However, in special cases, when a notch is perpendicular to the long axis of inclusions, comes to lamination effect or "lamination strengthening". Roughly explained, this straightening is primarily reflected in examination of ten connected samples of size 1 × 10 mm instead of a homogeneous sample test with a cross-section dimension 10 × 10 mm. As the lamination patterns become larger, a deformation of tube parts between the non-metallic inclusions are deformed to a greater extent under the plain stress condition. Apropos precisely described change of deformation, the total impact energy does not increase due to the present of non-metallic inclusions, the transient temperature toughness shifts to lower temperatures [18, 19].

As expected, the lower values of impact energy with a simulated tube welding cycle are quantitatively verified, in accordance with a literature. It was determined that there is a linear dependence between density (*i. e.* number) of pores in materials, and the energy that is absorbed during impact testing. Based on the value of impact strength, it was possible to show in this way that it can not only strengthen the fact regarding formation of micro pores due to creep, but also

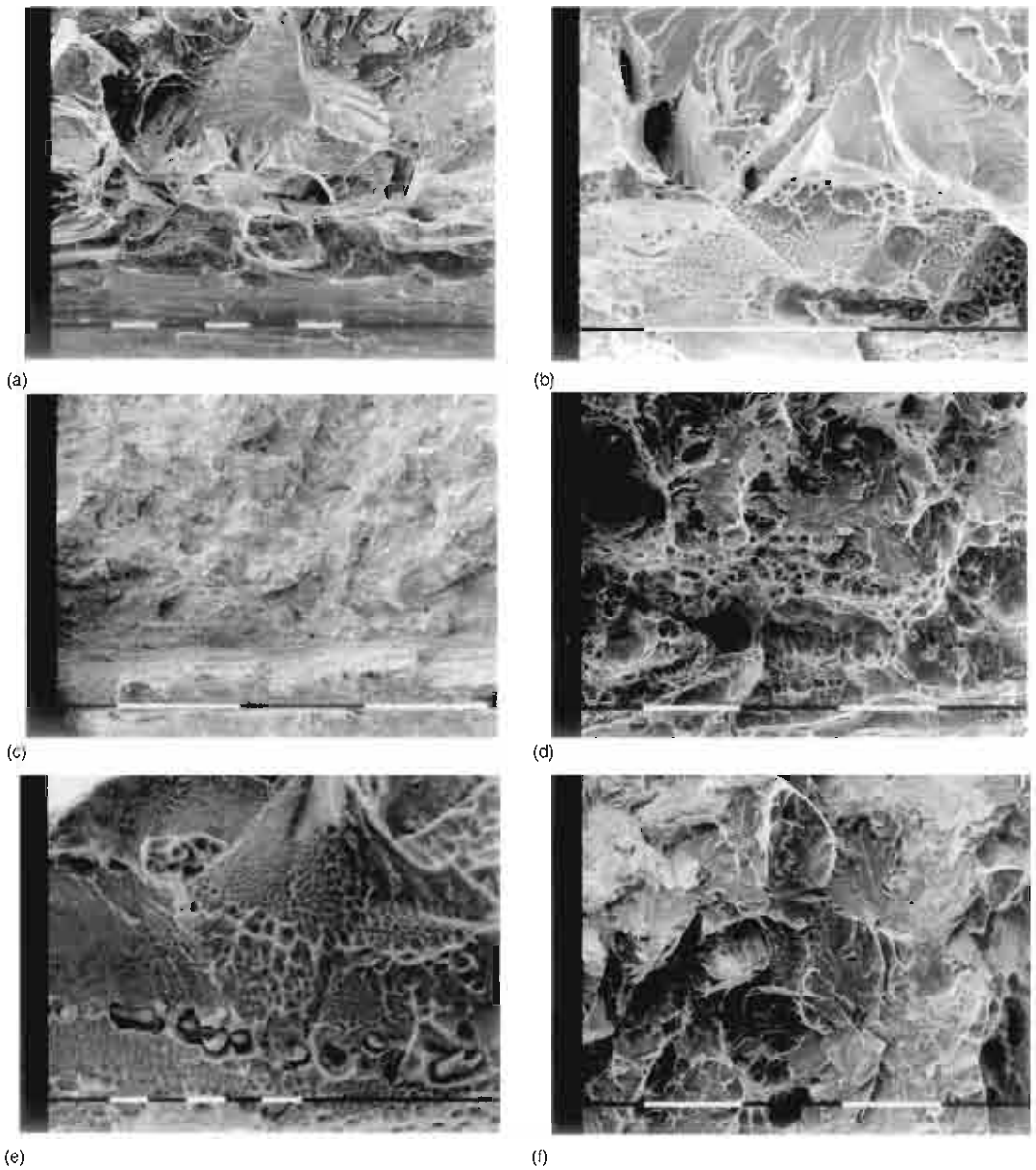

Figure 7. Fractography of samples from NP-L group;
(a) – single run welding, brittle fracture, ×30, (b) – single run welding, detail from previous fig., ductile fracture at the grain boundaries, ×100, (c) – multi run welding, detail fo the notch root with bands of sulfides, ×30, (d) – multi run welding, transition from notch root toward the center surfaces, brittle-ductile fracture, ×200, (e) – detail from figure d, non-metallic inclusions in th pits, ×400, (f) – multi run welding, brittle fracture, area of unstable crack growth, ×1000

to estimate the size of the volume in the unchanged structure. However, in the terms of industrial exploitation, the metal structure changes occurs with an accumulation of micro-pores, and the

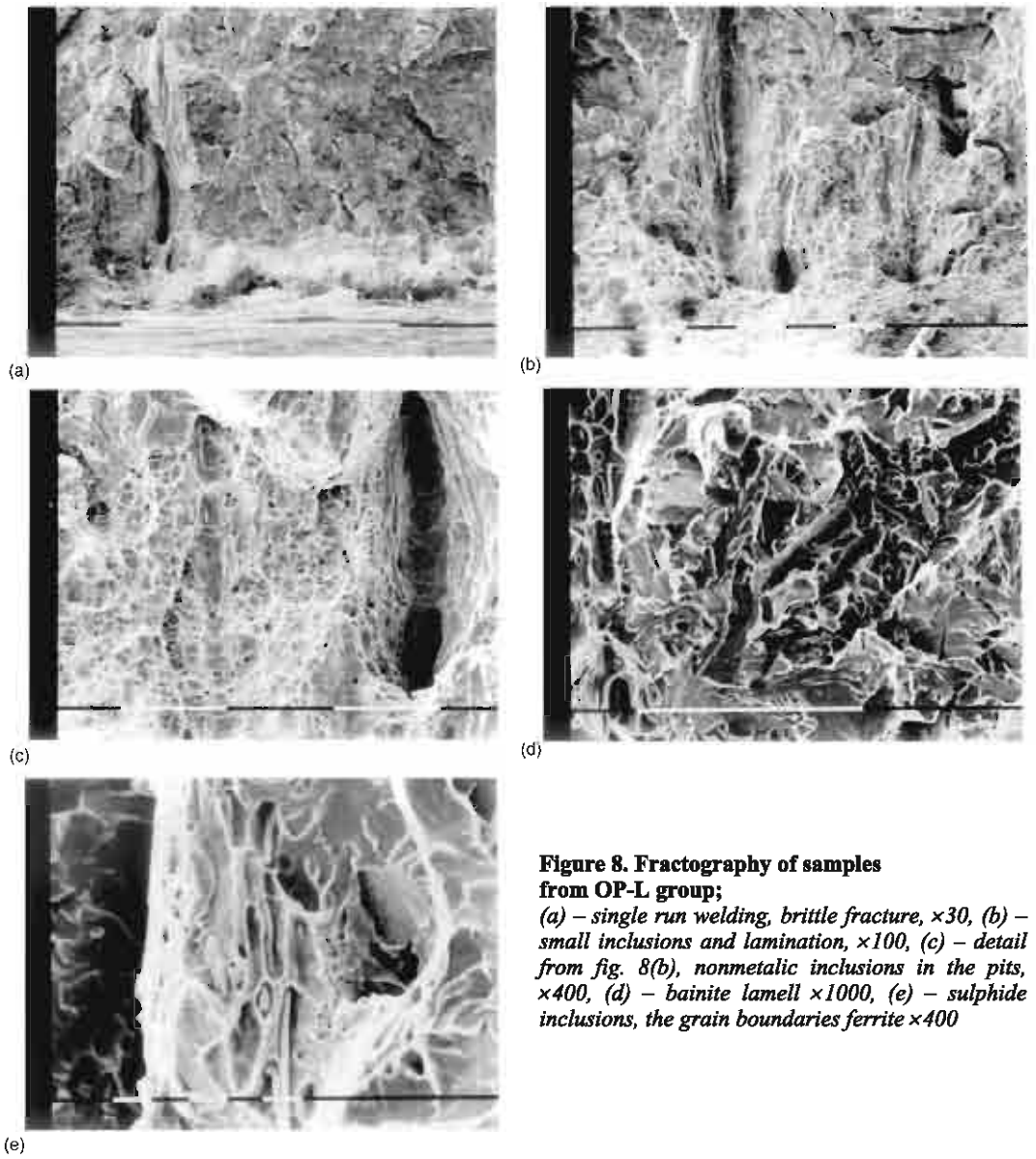

Figure 8. Fractography of samples from OP-L group;
(a) – single run welding, brittle fracture, ×30, (b) – small inclusions and lamination, ×100, (c) – detail from fig. 8(b), nonmetalic inclusions in the pits, ×400, (d) – bainite lamell ×1000, (e) – sulphide inclusions, the grain boundaries ferrite ×400

effects on reduction of impact strength is very difficult to separate [10]. Also, a great waste of steel from exploitation, (group OP), has been observed. This dissipation can be explained by the different proportion of ferrite on the grain boundaries, fine carbide network from sample to sample, and damages according to a sample result of scattering shown in fig. 9. Disparity in results, or greater dispersion, indicates entry into the area of transition temperature of toughness, which is typical for an extended time of exploration.

The microstructure, obtained by simulating multi run weld, corresponds to the expected. Particularly surprising fact is that the steel from exploitation, group OP, had more im-

pact energy value after the multi layer simulation then unused steal from group NP. As the microstructures are very similar in both groups, the only possible explanation is that steal from OP group is not near the end of its working life, which is consistent with data on sampled pipes.

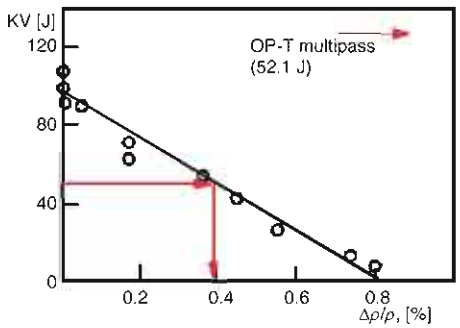

Figure 9. The change of the impact energy with an increased density of pores in 12H1MF

It is not uncommon that the microstructure obtained through simulation, on the total value of impact energy, has much greater impact with trace elements, which are rarely reveled with a standard classical titration volumetric analysis. In addition, it is known that the crack initiation does not occur on the interphase boundary between brittle and ductile phases. Brittle and ductile phases are not the only cause. Mixed microstructure in the simulated HAZ, the differences between the impact energy in the upper and lower bainite also affects strongly. In addition to these facts, it should have in mind that the package size has the biggest impact on the resilience of the upper bainite [20-22]. However, considering the HAZ phenomenon in terms of inclusions, of particular interest is the fact that "pure" inclusion practically does not exist (*e. g.* sulphide type). Even in a small percentage of "alloying" inclusions by the alloying elements present, there is a significant change in physical properties of inclusions, primary the melting temperature. Thus, in the steel, with low content of manganese and sulfur, complete sulfur is dissolved at 1240 °C allowing re-deposition of sulphide from austenite [23].

This re-precipitation of MnS is largely responsible for the appearance of overheating. MnS particle size in this case is about 1 μm, a distance between is about 2 μm, and the separation occurs at the grain boundaries. The structure formed in this way is susceptible to breakage by the so-called grains pseudo-boundaries, or fracture (*e. g.* when examining impact energy) can occur at the borders of the former austenitic grain. In simulations of HAZ steel 2.25 Cr1Mo, this phenomenon has been observed already at achieving 1200 °C. Obviously this structure, especially from the standpoint of toughness, is very unfavorable and difficult to remove. By cycling temperature trough A_{C1}, which correspond multi layer welding, grain boundaries can be moved from this isolated, finely dispersed sulphide inclusions [24]. This is a re-allocation of highly dispersed non-metallic inclusions during the cooling, and after reaching the maximum cycle. As shown in fig. 8(b), inclusions were dispersed in the former austenite grain boundaries. The intercrystal fracture has occurred precisely at these boundaries during the examination of the impact energy.

Conclusions

Based on analysis of test results in this study obtained by thermal cycling heat simulator we can conclude the following.

- The study found that the difference between the impact energy simulation between single run welding and multi run welding was higher in the case of used materials such as group of OP samples, than in fresh material of the group NP.
- A higher impact energy values within a group in test tubes from the longitudinal than the transverse direction were detected.
- The presence of non-metallic inclusions is substantially affecting the character of fracture.

- The unstable fracture was also observed in OP-L and NP-L group samples, with relatively high values of impact energy and simulated multi run welding.
- A significant change of a fracture mechanism was observed in OP-L group samples in references to exploitation steel simulation. In the simulation of the single layer welding almost entire absorbed energy is used on the crack initiation, while the propagation energy is quite small. In a simulation of multi run welding, most of the total absorbed energy is wasted on the propagation energy.
- It is possible to obtain an optimal impact energy values in multi run welding by changing the welding parameters for each cycle, without compromising other mechanical properties of HAZ.

Acknowledgment

This work has been supported by the Ministry of Science and Technological Development of the Republic of Serbia under Projects: TR 35029 and TR 34015.

References

[1] Viswanathan, R., Damage Mechanisms and Life Assessment of High Temperature Components, ASM International, Geauga County, O., USA, 1989, pp. 15-17
[2] Badet, H., Maintenance of High-Pressure / High-Temperature Piping in Fossil Fueled Power Plants, *Alsthom Review, 9* (1987), pp. 17-27
[3] Spera, D. A., What is Thermal Fatigue? Thermal Fatigue of Materials and Components, ASTM Special Technical Publication 612, 1976, pp. 3-9
[4] Totten, G., *et al.*, Handbook of Residual Stress and Deformation of Steel, ASM International., O., USA, 2000, pp. 392-396
[5] Shipley, R. J. Becker, W. T., ASM Handbook Volume 11 Failure Analysis and Prevention, ASM International, Geauga County, O., USA, 2002, pp. 2686-2739
[6] Russel, H. Jones, *et al.*, Stress- Corrosion Cracking Materials: Performance and Evaluation, ASM International., Geauga County, O., USA, 1993
[7] Landrum, J. R., Fundamentals of Design for Corrosion Control – A Corrosion Aid to the Designer, NACE, Houston., Tex., USA, 1989
[8] Singer J. G., Combustion Fossil Power Systems, *Combustion Engineering, Inc.,* Windsor, Conn., USA, 1991
[9] Riedel, H., Fracture at High Temperatures, Springer-Verlag, Heidelberg, Berlin, 1987
[10] Chadek, Y., Creep of Metallic Materials (Russian translation), Mir Publishers, Moscow, 1987
[11] Gooch, D. J., Remnant Creep Life Prediction in Ferritic Materials, in: Comprehensive Structural Integrity, Vol. 5, Creep and High Temperature Failures, Elsevier Pergamon, London, 2003, pp. 309-359
[12] Milović, Lj., *et al.*, Study of the Simulated Heat Affected Zone of Creep Resistant 9-12% Advanced Chromium Steel, *Materials and Manufacturing Processes, 23* (2008), 6, pp. 597-602
[13] Milović, Lj., Significance of Cracks in the Heat Affected Zone of Steels for Elevated Temperature Application, *Structural Integrity and Life, 8* (2008), 1, pp. 55-64
[14] Gliha, V., *et al.*, Fracture Resistance of Simulated Heat Affected Zone Areas in HSLA Structural Steel, *Science and Technology of Welding and Joining, 9* (2004), 5, pp. 399-406
[15] Dolby, R., E., Fracture Toughness Comparison of Weld HAZ and Thermally Simulated Microstructures, *Metal Construction and British Welding Journal, 4* (1972), 5, pp. 59-63
[16] Odanović, Z., Numerical Modeling of Heat Transfer in Arc Welding of Steel and Anticipation of Possible Effects on the Heat Affected Zone, Ph. D. thesis, Faculty of Technology and Metallurgy, University of Belgrade, Belgrade, 1993, pp. 39-43
[17] ***, GOST 20072-74: Heat Resisting Steel, Specification
[18] Kucera, J., *et al.*, On the Fracture of Laminated Charpy V Notch Specimens, *Proceedings*, AEFM, Rome, 1980, pp. 515-525

[19] Garde, A. M., Weiss, V., Brittle Crack Initiation at the Elasic-Plastic Interface, *Met. Trans. A, 3* (1971-1972), pp. 2811-2817, pp. 2811-2817
[20] Naylor, J. P., Krahe, P. R., The Effect of Bainitic Packet Size on Toughness, *Met. Trans. A, 5* (1974), pp. 1699-1701, pp. 1699-1701
[21] Bhadeshia, H. K. D. H, Bainite in Steels, The Institute of Materials, London, 1992, pp. 246-247
[22] Kiessling, R., Lange.N., Non-Metalic Inclusions in Steel, The Institute of Materials, London, 1997, Section P, pp. 54-73
[23] Pugh, S. F., An Introduction to Grain Boundary Fracture in Metals, The Institute of Metals, London, 1991, pp. 53; 89
[24] Lazić, V. N., *et al.*, Energetic Analysis of Hard Facing and Weld Cladding of an Air Powered Drop Hammer Damaged Ram, *Thermal Science, 14* (2010), Suppl. pp. S269-S284

Paper submitted: October 6, 2011
Paper revised: December 6, 2011
Paper accepted: December 11, 2011